JOURNAL OF COMPUTATIONAL PHYSICS 26, 390–407 (1978)

A Semi-Implicit Method for Two-Phase Fluid Dynamics

D. R. LILES AND WM. H. REED*

Los Alamos Scientific Laboratory, University of California,
P. O. Box 1663, Los Alamos, New Mexico 87545

Received October 18, 1976; revised February 24, 1977

A new technique is developed for solving the equations of two-phase fluid dynamics. This technique involves a semi-implicit differencing of the field equations and a variation of the Newton Gauss Seidel iterative method for solving at each time level the resulting system of algebraic equations. Although the technique can be applied to any of several sets of equations representing two-phase flow, including the two-fluid equations, numerical results are presented here for the drift-flux approximation in one dimension. Significant advantages of the method are its stability, ease of programming for complicated flow networks, and ease of extension to problems in two or three dimensions.

1. INTRODUCTION

Two-phase fluid dynamics has been described by several sets of equations ranging in complexity from a simple homogeneous equilibrium model to a very complicated two-fluid model involving a separate pressure for each phase [1, 2]. The methods developed in this paper have been applied to both simple and complex models of two-phase flow. The immediate application of the present work is to the analysis of the safety of nuclear reactors. In the unlikely event of breach of the primary coolant system, a two-phase mixture of water and steam is ejected from the break. The central problem, then, is the prediction of the state of the fluid in the primary system as a function of time so that adequate cooling of the reactor core can be ensured. It is widely believed that an accurate prediction of the fluid state requires consideration of the relative motion of the vapor and liquid phases and consideration of certain nonequilibrium thermodynamic effects such as finite-rate phase change. Perhaps the simplest model capable of incorporating such effects is the drift-flux model, and we have chosen this model to demonstrate our method.

In Section 2 of this paper we present the field and constitutive equations of the drift-flux model. Section 3 contains a description of difference techniques and iterative solution algorithms that have been used to solve these equations. In practice this solution procedure has proved to be stable and capable of generating solutions in problems where other schemes have failed. The method converges rapidly for

* Work performed under the auspices of the U.S. Nuclear Regulatory Commission.

0021-9991/78/0263–0390$02.00/0

reasonable error tolerances and is easily extended to two- or three-dimensional geometries. Section 4 contains numerical results illustrating the capabilities of this method for several representative problems.

2. The Drift-Flux Model

A. *Field Equations*

The drift-flux field equations for a two-phase mixture consist of two mass conservation equations, one momentum conservation equation, and one internal energy equation [1, 2]. The internal energy equation is replaced in some formulations by an entropy or an enthalpy equation. In this paper, we utilize the following forms of these four partial differential equations:

Mixture mass conservation

$$\frac{\partial \rho_m}{\partial t} + \frac{\partial}{\partial z}(\rho_m v_m) = 0. \tag{1}$$

Vapor mass conservation

$$\frac{\partial}{\partial t}(\alpha\rho_v) + \frac{\partial}{\partial z}(\alpha\rho_v v_m) + \frac{\partial}{\partial z}\left[\frac{\alpha\rho_v(1-\alpha)\,\rho_l v_r}{\rho_m}\right] = \Gamma. \tag{2}$$

Mixture momentum conservation

$$\frac{\partial}{\partial t}(\rho_m v_m) + \frac{\partial}{\partial z}(\rho_m v_m^2) + \frac{\partial}{\partial z}\left[\frac{(1-\alpha)\,\rho_l\alpha\rho_v v_r^2}{\rho_m}\right] + \frac{\partial p}{\partial z} + \rho_m g_z + \tau = 0. \tag{3}$$

Mixture specific internal energy conservation

$$\frac{\partial}{\partial t}(\rho_m e_m) + \frac{\partial}{\partial z}(\rho_m e_m v_m) + \frac{\partial}{\partial z}\left[\frac{(1-\alpha)\,\rho_l\alpha\rho_v v_r(e_v - e_l)}{\rho_m}\right]$$
$$+ p\frac{\partial v_m}{\partial z} + p\frac{\partial}{\partial z}\left[\frac{\alpha(1-\alpha)\,v_r(\rho_l - \rho_v)}{\rho_m}\right] = q. \tag{4}$$

Variables appearing in the above equations have the following meanings:

ρ_m	mixture density
ρ_v	vapor density (microscopic)
ρ_l	liquid density (microscopic)
α	vapor volume fraction
v_m	mixture velocity
v_r	relative velocity between phases
e_v	vapor specific internal energy

e_l liquid specific internal energy
e_m mixture specific internal energy
Γ vapor production rate due to phase change
p pressure
g_z force of gravity in the z direction
τ wall friction
q heat source
T_l liquid temperature
T_v vapor temperature
T_s saturation temperature

The three temperatures listed above do not appear in Eqs. (1)–(4) but do appear in the constitutive equations below. They have been included in the above list for completeness. At present, we have written four equations for the seventeen variables listed above. The gravitational term g_z is a function of only the independent variable z and does not depend on the state variables. We assume that $g_z(z)$ is known from the geometrical configuration of the particular system under study. To effect closure, we must therefore specify twelve additional relationships among these variables. Two relationships may be obtained from basic definitions of mixture quantities. These definitions are:

1. Definition of ρ_m :

$$\rho_m = (1 - \alpha)\,\rho_l + \alpha\rho_v\,. \tag{5}$$

2. Definition of e_m :

$$e_m = \frac{(1 - \alpha)\,\rho_l e_l + \alpha\rho_v e_v}{\rho_m}\,. \tag{6}$$

The remaining ten relationships are discussed in the following section.

B. *Constitutive Equations*

We refer to the ten additional relationships needed for closure of the system of equations as constitutive equations. A general form for each of these equations is presented below; specific forms used in our computations are presented in the section on numerical results.

1. *Thermal equation of state for the liquid.* We assume that a relationship giving the liquid density as a function of pressure and liquid internal energy is available:

$$\rho_l = \rho_l(p, e_l). \tag{7}$$

This relationship must apply for a superheated as well as a subcooled liquid.

2. *Thermal equation of state for the vapor.* The vapor thermal equation of state is analogous to that of the liquid:

$$\rho_v = \rho_v(p, e_v). \tag{8}$$

This relationship must apply for both superheated and subcooled vapor.

3. *Caloric equation of state for the liquid.* This equation is assumed to take the form

$$T_l = T_l(p, e_l). \tag{9}$$

We further assume that this relationship can be inverted to obtain

$$e_l = e_l(p, T_l). \tag{10}$$

4. *Caloric equation of state for the vapor.* The vapor caloric equation of state is similar to that of the liquid:

$$T_v = T_v(p, e_v). \tag{11}$$

We again assume inversion is possible, yielding

$$e_v = e_v(p, T_v). \tag{12}$$

5. *Wall heat source.* The heat source term in the energy equation is assumed to be of the form

$$q = hA(T_w - T_f), \tag{13}$$

where A is the wall area, T_w is the wall temperature, and T_f is a fluid temperature, possibly T_l or T_v or some average temperature. The heat transfer coefficient h is obtained from correlations involving the fluid properties and the wall temperatures.

6. *Wall friction.* The wall friction term takes the form

$$\tau = c(\rho_m v_m \mid v_m \mid /2D), \tag{14}$$

where D is the hydraulic diameter and c is a friction multiplier depending strongly upon the vapor fraction α and other fluid properties.

7. *Relative velocity correlation.* We assume the existence of a relationship specifying the relative velocity in terms of the other state variables. This relationship will usually be strongly dependent on an assumed flow topology.

8. *Rate of phase change.* The rate of phase change Γ must be specified as a function of the other variables. Various models employing equilibrium or nonequilibrium assumptions are possible.

9. *Saturation curve.* A saturation curve of the form

$$T_s = T_s(p)$$

must be specified. The saturation temperature provided by this curve enters the phase change expression of item 8 above.

10. *A thermal constraint.* The drift-flux field equations provide only a single mixture energy equation for the two specific internal energies e_l and e_v. An additional thermal constraint is necessary to partition the mixture energy into the liquid and vapor phases. A variety of such constraints is possible, the simplest of which is thermal equilibrium between phases. Another possibility is the assumption that either the vapor or the liquid is at saturation, depending upon whether vaporization or condensation is occurring.

3. The Difference Scheme

The convective terms in Eqs. (1)–(4) have been written in a divergence or conservation form. Because there are large sources and sinks of momentum in a nuclear reactor (pumps, orifices, etc.), we will not attempt to ensure that our difference schemes be rigorously conservative in the treatment of momentum convection. Therefore, we choose to rewrite Eq. (3) in a nonconservative form that is more convenient in our applications. Multiplying Eq. (1) by v_m and subtracting from Eq. (3) yields the equation

$$\frac{\partial v_m}{\partial t} + v_m \frac{\partial v_m}{\partial z} + \frac{1}{\rho_m} \frac{\partial}{\partial z} \left[\frac{(1-\alpha)\, \rho_l \alpha \rho_v v_r^2}{\rho_m} \right] + \frac{1}{\rho_m} \frac{\partial p}{\partial z} + g_z + \frac{\tau}{\rho_m} = 0. \quad (15)$$

The finite-difference form of Eq. (15) exhibits certain simplifications over that of Eq. (3). We use Eqs. (1), (2), (4) and (15) throughout the following analysis.

The mesh cell configuration and the labeling conventions for cell edges and cell centers are depicted in Fig. 1. The mass and energy equations are differenced over the mesh cells indicated by solid lines in Fig. 1; the momentum equation is differenced over the dashed mesh cells. This forms a staggered spatial difference scheme which has been used by many others for the solution of both single-phase [3] and multiphase [4, 5] problems. The resulting difference equations are

$$\frac{(\rho_m)_i^{n+1} - (\rho_m)_i^n}{\Delta t} + \frac{(\rho_m)_{i+\frac{1}{2}}^n (v_m)_{i+\frac{1}{2}}^{n+1} - (\rho_m)_{i-\frac{1}{2}}^n (v_m)_{i-\frac{1}{2}}^{n+1}}{\Delta z} = 0, \quad (16)$$

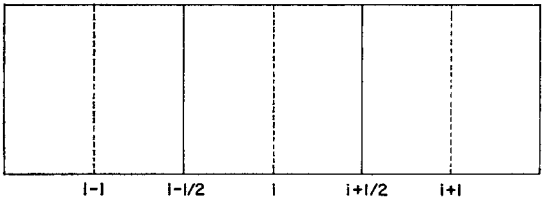

FIG. 1. Mesh cell labeling convention.

$$\frac{(\alpha\rho_v)_i^{n+1} - (\alpha\rho_v)_i^n}{\Delta t} + \frac{(\alpha\rho_v)_{i+\frac{1}{2}}^n (v_m)_{i+\frac{1}{2}}^{n+1} - (\alpha\rho_v)_{i-\frac{1}{2}}^n (v_m)_{i-\frac{1}{2}}^{n+1}}{\Delta z}$$
$$+ \frac{1}{\Delta z}\left\{\left[\frac{(1-\alpha)\rho_l\alpha\rho_v v_r}{\rho_m}\right]_{i+\frac{1}{2}}^n - \left[\frac{(1-\alpha)\rho_l\alpha\rho_v v_r}{\rho_m}\right]_{i-\frac{1}{2}}^n\right\} = \Gamma, \tag{17}$$

$$\frac{(v_m)_{i+\frac{1}{2}}^{n+1} - (v_m)_{i+\frac{1}{2}}^n}{\Delta t} + (v_m)_{i+\frac{1}{2}}^n \left[\frac{(v_m)_{i+1}^n - (v_m)_i^n}{\Delta z}\right]$$
$$+ \frac{1}{(\rho_m)_{i+\frac{1}{2}}^n \Delta z}\left\{\left[\frac{(1-\alpha)\rho_l\alpha\rho_v v_r^2}{\rho_m}\right]_{i+1}^n - \left[\frac{(1-\alpha)\rho_l\alpha\rho_v v_r^2}{\rho_m}\right]_i^n\right\}$$
$$+ \frac{1}{(\rho_m)_{i+\frac{1}{2}}^n}\left(\frac{p_{i+1}^{n+1} - p_i^{n+1}}{\Delta z}\right) + (g_z)_{i+\frac{1}{2}} + \left(\frac{\tau}{\rho_m}\right)_{i+\frac{1}{2}} = 0, \tag{18}$$

$$\frac{(\rho_m e_m)_i^{n+1} - (\rho_m e_m)_i^n}{\Delta t} + \frac{(\rho_m e_m)_{i+\frac{1}{2}}^n (v_m)_{i+\frac{1}{2}}^{n+1} - (\rho_m e_m)_{i-\frac{1}{2}}^n (v_m)_{i-\frac{1}{2}}^{n+1}}{\Delta z}$$
$$+ \frac{1}{\Delta z}\left\{\left[\frac{(1-\alpha)\rho_l\alpha\rho_v(e_v - e_l)}{\rho_m} v_r\right]_{i+\frac{1}{2}}^n\right.$$
$$\left. - \left[\frac{(1-\alpha)\rho_l\alpha\rho_v(e_v - e_l)}{\rho_m} v_r\right]_{i-\frac{1}{2}}^n\right\} + p_i^{n+1}\left[\frac{(v_m)_{i+\frac{1}{2}}^{n+1} - (v_m)_{i-\frac{1}{2}}^{n+1}}{\Delta z}\right]$$
$$+ \frac{p_i^n}{\Delta z}\left\{\left[\frac{\alpha(1-\alpha)(\rho_l - \rho_v)}{\rho_m} v_r\right]_{i+\frac{1}{2}}^n - \left[\frac{\alpha(1-\alpha)(\rho_l - \rho_v)}{\rho_m} v_r\right]_{i-\frac{1}{2}}^n\right\} = q. \tag{19}$$

In the above equations the superscripts n and $n + 1$ refer to time levels, Δt and Δz are mesh spacings in time and space, respectively, and Δz is assumed to be a constant, although this is not a fundamental restriction of the method.

The above difference equations are semi-implicit. We note that the convective terms in the mass and energy equations, the pressure gradient term in the momentum equation, and the compressible work term in the energy equation all contain terms evaluated at the new time level. All other terms in these equations have been evaluated at the old time level, with the exception of the phase transition rate Γ, the wall friction term τ, and the wall heat source q. We have not indicated in Eqs. (16)–(19) the time level at which these three terms are to be evaluated. Each of these terms may be a complicated function of the fluid state. Once this function is specified, it is usually possible to evaluate certain parts at the new time. Because these terms represent important, if not dominant, source or loss mechanisms, it is usually advantageous to treat them in as implicit a manner as possible. The specific manner in which these terms have been evaluated in the present work is discussed in the section on numerical results.

The degree of implicitness exhibited in Eqs. (16)–(19) has been deliberately chosen to meet several objectives. First, because the nuclear reactor safety problems to which this method will be applied involve a wide range of fluid velocities, from

sonic to far subsonic, we seek a method that is not limited by the classical stability condition $(v + c)\,\Delta t/\Delta z < 1$, where c is the sound speed. Numerical tests indicate that the method of Eqs. (16)–(19) possesses an approximate stability criterion of the form $v_m\,\Delta t/\Delta z < 1$, provided that relative velocities v_r are smaller than mixture velocities, so that time steps consistent with fluid velocities may be taken. Second, the above difference equations represent a near-maximum degree of implicitness consistent with a straightforward, easily programmed, and rapidly convergent solution strategy for the resulting system of nonlinear algebraic equations. Such a solution strategy is presented in the next section. Third, the low-order accuracy provided by this scheme is probably sufficient for reactor safety problems in which basic constitutive equations are imprecise.

The above difference equations, with the addition of appropriate constitutive relationships, do not form a complete set of equations for the variables at all node positions. These difference equations must be supplemented by additional relationships among variables at the edges and centers of mesh cells. We use the following relationships, which produce a "weighted donor cell" difference scheme that is particularly stable (see [4, 5], for example):

$$\begin{aligned}
\rho_{i+\frac{1}{2}} &= \left(\frac{1+\beta_{i+\frac{1}{2}}}{2}\right)\rho_i + \left(\frac{1-\beta_{i+\frac{1}{2}}}{2}\right)\rho_{i+1}\,,\\
\alpha_{i+\frac{1}{2}} &= \left(\frac{1+\beta_{i+\frac{1}{2}}}{2}\right)\alpha_i + \left(\frac{1-\beta_{i+\frac{1}{2}}}{2}\right)\alpha_{i+1}\,,\\
e_{i+\frac{1}{2}} &= \left(\frac{1+\beta_{i+\frac{1}{2}}}{2}\right)e_i + \left(\frac{1-\beta_{i+\frac{1}{2}}}{2}\right)e_{i+1}\,,\\
v_i &= \left(\frac{1+\beta_i}{2}\right)v_{i-\frac{1}{2}} + \left(\frac{1-\beta_i}{2}\right)v_{i+\frac{1}{2}}\,.
\end{aligned} \tag{20}$$

In the above equations, ρ and e stand for ρ_m, ρ_l, or ρ_v and e_m, e_l, or e_v, as appropriate. The variable v may be understood as either v_m or v_r. The weighting parameter β, which varies between -1 and $+1$, can be selected in a veriety of ways. The specification $\beta = 0$ yields the more accurate but less stable central difference technique. On the other hand, if β is chosen as

$$\beta_{i+\frac{1}{2}} = v_{i+\frac{1}{2}}/|\,v_{i+\frac{1}{2}}\,| \equiv \operatorname{sign}(v_{i+\frac{1}{2}}),$$

then full donor cell differencing is obtained. This technique is very stable but first-order accurate. A number of schemes representing compromises between central and full donor cell differencing are possible.

4. The Solution Procedure

The difference equations (16)–(19) in conjunction with the donor cell relationships of Eq. (20) and the constitutive equations of Section 2B represent a nonlinear algebraic system of equations for all mesh variables at the new time level. We have developed

a new method, which we will call the Newton Block Gauss Seidel (NBGS) method, for solving this system of equations. The NBGS method is a variation of the Newton Gauss Seidel method discussed by Ortega and Reinboldt [6]. In theory, the method represents a primary Newton iteration on the original nonlinear system coupled with a secondary Block Gauss Seidel iteration for solving the linear system generated at each stage of the Newton iteration. The NBGS method, as implemented in this paper, involves a single step of the secondary iteration for each step of the primary one. A block inversion technique is used instead of the standard Gauss Seidel method because of the strong coupling that exists in the field equations. The phase change term Γ is one of the most important coupling terms in these equations, since it represents vapor production which can change the mixture compressibility by orders of magnitude and thus strongly affect the fluid motion. The block technique allows this dominant term to be computed in a more implicit manner than the Kachina [4] procedure. In the remainder of this section, we present a detailed description of how NBGS works in one dimension and an indication of how the technique can be extended to two or three dimensions.

The NBGS technique can be divided into the following four stages.

1. All equations, including both difference and constitutive equations, are linearized around the latest iterate values of the unknowns.

2. All unknowns appearing in the difference equations, except α, p, v_{m}, and e_l, are eliminated by using the linearized definitions and constitutive equations. This yields a linear system of equations for the four variables α, p, v_{m}, and e_l at all mesh points.

3. These equations are then used to generate new values for α, p, v_{r}, and e_l at all mesh cells. In this process, some terms in the equations are evaluated using pressures at the old iterate.

4. The remaining unknowns are determined from α, p, v_{m}, and e_l by using the appropriate definitions and constitutive equations. We emphasize that the full nonlinear equations are used in this stage of the computation.

The above choice of four fundamental unknowns, one for each partial differential equation, is not unique. We might, for example, have chosen to solve for two densities instead of pressure and vapor fraction. There are three reasons for the particular choice we have made here. First, the pressure may be a continuous function of distance across a contact discontinuity (a slug of liquid next to a vapor bubble), but the density is not continuous. Second, the pressure equation of state is a very sensitive function of the density for an all-liquid system. Thus, if density were a fundamental unknown small errors in the density would produce large errors in pressure. This leads to a less stable algorithm. Third, the thermodynamic relationships can be handled in a more straightforward manner if pressure and an energy or a temperature are available.

We now give a detailed description of the NBGS technique. We demonstrate the

manner in which the first two stages of this technique are carried out by using the mixture mass conservation equation as an example:

$$\frac{(\rho_m)_i^{n+1} - (\rho_m)_i^n}{\Delta t} + (\rho_m)_{i+\frac{1}{2}}^n (v_m)_{i+\frac{1}{2}}^{n+1} - (\rho_m)_{i-\frac{1}{2}}^n (v_m)_{i-\frac{1}{2}}^{n+1} = 0. \tag{21}$$

We note that this equation is already linear in the new time variables $(\rho_m)_i^{n+1}$ and $(v_m)_{i+\frac{1}{2}}^{n+1}$. We want to replace the densities $(\rho_m)_i^{n+1}$ in the above equation by the four fundamental unknowns listed above. We begin by using the definition of Eq. (5),

$$\rho_m = (1 - \alpha)\,\rho_l + \alpha\rho_v\,, \tag{22}$$

the thermal equations of state,

$$\rho_l = \rho_l(p, e_l), \tag{23}$$

$$\rho_v = \rho_v(p, e_v), \tag{24}$$

and a thermal constraint as discussed in Section 2B. Let us assume for definiteness that an equal-temperature assumption is used:

$$T_v = T_l\,. \tag{25}$$

In this case it is also necessary to introduce the caloric equations of state:

$$e_l = e_l(p, T_l), \tag{26}$$

$$e_v = e_v(p, T_v). \tag{27}$$

The above six equations, (22)–(27), determine the six quantities ρ_m, ρ_l, ρ_v, e_v, T_l, and T_v in terms of α, p, and e_l. Depending upon the form of the equations of state, this relationship is quite complicated. Because we want an analytic relationship between the density ρ_m and the fundamental unknowns, we linearize these six equations and eliminate the five extraneous variables ρ_l, ρ_v, e_v, T_l, and T_v. For the moment, we indicate the point about which these equations are linearized by a tilde. The linear forms of Eqs. (22)–(27) are listed below:

$$\rho_m = \tilde{\rho}_m + (\tilde{\rho}_v - \tilde{\rho}_l)(\alpha - \tilde{\alpha}) + (1 - \tilde{\alpha})(\rho_l - \tilde{\rho}_l) + \tilde{\alpha}(\rho_v - \tilde{\rho}_v), \tag{28}$$

$$\rho_l = \tilde{\rho}_l + \frac{\partial\tilde{\rho}_l}{\partial p}(p - \tilde{p}) + \frac{\partial\tilde{\rho}_l}{\partial e_l}(e_l - \tilde{e}_l), \tag{29}$$

$$\rho_v = \tilde{\rho}_v + \frac{\partial\tilde{\rho}_v}{\partial p}(p - \tilde{p}) + \frac{\partial\tilde{\rho}_v}{\partial e_v}(e_v - \tilde{e}_v), \tag{30}$$

$$T_v = T_l\,, \tag{31}$$

$$e_l = \tilde{e}_l + \frac{\partial\tilde{e}_l}{\partial p}(p - \tilde{p}) + \frac{\partial\tilde{e}_l}{\partial T_l}(T_l - \tilde{T}_l), \tag{32}$$

$$e_v = \tilde{e}_v + \frac{\partial\tilde{e}_v}{\partial p}(p - \tilde{p}) + \frac{\partial\tilde{e}_v}{\partial T_v}(T_v - \tilde{T}_v). \tag{33}$$

The eight derivatives appearing in Eqs. (28)–(33) represent derivatives of the equation-of-state functions appearing on the right-hand sides of Eqs. (23), (24), (26), and (27). These derivatives are evaluated at the points $(\tilde{p}, \tilde{e}_v)$ and $(\tilde{p}, \tilde{e}_l)$ as is appropriate. We now use Eqs. (31)–(33) and the additional assumption that $\tilde{T}_l = \tilde{T}_v$ to obtain the following relationship between e_l and e_v :

$$\frac{\partial \tilde{e}_v}{\partial T_v}\left[e_l - \tilde{e}_l - \frac{\partial \tilde{e}_l}{\partial p}(p - \tilde{p})\right] = \frac{\partial \tilde{e}_l}{\partial T_l}\left[e_v - \tilde{e}_v - \frac{\partial \tilde{e}_v}{\partial p}(p - \tilde{p})\right]. \tag{34}$$

Inserting Eqs. (29) and (30) in Eq. (28), we obtain

$$\rho_m = \tilde{\rho}_m + (\tilde{\rho}_v - \tilde{\rho}_l)(\alpha - \tilde{\alpha}) + (1 - \tilde{\alpha})\left[\frac{\partial \tilde{\rho}_l}{\partial p}(p - \tilde{p}) + \frac{\partial \tilde{\rho}_l}{\partial e_l}(e_l - \tilde{e}_l)\right]$$
$$+ \tilde{\alpha}\left[\frac{\partial \tilde{\rho}_v}{\partial p}(p - \tilde{p}) + \frac{\partial \tilde{\rho}_v}{\partial e_v}(e_v - \tilde{e}_v)\right]. \tag{35}$$

Finally, we use Eq. (34) to eliminate e_v in Eq. (35), giving

$$\rho_m = \tilde{\rho}_m + (\tilde{\rho}_v - \tilde{\rho}_l)(\alpha - \tilde{\alpha}) + (1 - \tilde{\alpha})\left[\frac{\partial \tilde{\rho}_l}{\partial p}(p - \tilde{p}) + \frac{\partial \tilde{\rho}_l}{\partial e_l}(e_l - \tilde{e}_l)\right]$$
$$+ \tilde{\alpha}\left\{\frac{\partial \tilde{\rho}_v}{\partial p}(p - \tilde{p}) + \frac{\partial \tilde{\rho}_v}{\partial e_v}\frac{\partial \tilde{T}_l}{\partial e_l}\frac{\partial \tilde{e}_v}{\partial T_v}\left[(e_l - \tilde{e}_l) - \frac{\partial \tilde{e}_l}{\partial p}(p - \tilde{p})\right]\right.$$
$$\left. + \frac{\partial \tilde{\rho}_v}{\partial e_v}\frac{\partial \tilde{e}_v}{\partial p}(p - \tilde{p})\right\}. \tag{36}$$

The above expression is a linear relationship between the mixture density and three fundamental unknowns α, p, and e_l.

To complete steps 1 and 2 of the NBGS technique for the mixture mass conservation, we use Eq. (36) to eliminate the mixture density $(\rho_m)_i^{n+1}$ appearing in Eq. (21). Introducing the superscripts k and $k+1$ to indicate successive iterative approximations to variables at the new time and evaluating the tilde quantities in Eq. (36) at the kth iterate, we obtain

$$(\rho_m)_i^k - (\rho_m)_i^n + [(\rho_v)_i^k - (\rho_l)_i^k](\alpha_i^{k+1} - \alpha_i{}^k)$$
$$+ \left[(1 - \alpha_i{}^k)\frac{\partial \rho_l{}^k}{\partial p} + \alpha_i{}^k\left(\frac{\partial \rho_v{}^k}{\partial p} - \frac{\partial \rho_v{}^k}{\partial e_v}\frac{\partial e_v{}^k}{\partial T_v}\frac{\partial T_l{}^k}{\partial e_l}\frac{\partial e_l{}^k}{\partial p} + \frac{\partial \rho_v{}^k}{\partial e_v}\frac{\partial e_v{}^k}{\partial p}\right)\right]$$
$$\times (p_i^{k+1} - p_i{}^k) + \left[(1 - \alpha_i{}^k)\frac{\partial p_l{}^k}{\partial e_l} + \alpha_i\frac{\partial p_v{}^k}{\partial e_v}\frac{\partial T_l{}^k}{\partial e_l}\frac{\partial e_v{}^k}{\partial T_v}\right][(e_l)_i^{k+1} - (e_l)_i^k]$$
$$+ \frac{\Delta t}{\Delta z}[(\rho_m)_{i+\frac{1}{2}}^n (v_m)_{i+\frac{1}{2}}^{k+1} - (\rho_m)_{i-\frac{1}{2}}^n (v_m)_{i-\frac{1}{2}}^{k+1}] = 0. \tag{37}$$

In the above equation we have used the convention that

$$u^{n+1,k} = u^k,$$

since it is always understood that we are developing successive approximations to new time quantities. This equation is a linear equation for the five quantities α_i^{k+1}, p_i^{k+1}, $(e_l)_i^{k+1}$, $(v_m)_{i+\frac{1}{2}}^{k+1}$, and $(v_m)_{i-\frac{1}{2}}^{k+1}$. By repeating the above procedure for the three remaining difference equations, we can obtain a complete set of linear algebraic equations for the four fundamental unknowns at all mesh cells. Because these equations are complicated but easily derived by following the procedures outlined above, we will not write them in detail here.

We begin our description of the third stage of the NBGS technique by indicating in Fig. 2 the structure of the linear system derived as discussed above. In this figure we have ordered the mesh variables in a particular manner and have indicated all nonzero entries in the coefficient matrix by an X. It is clear from this figure that these nonzero entries can be grouped into a pattern of overlapping 5×5 blocks. Each of these blocks represents coefficients of unknowns associated with a single solid mesh cell (see Fig. 1), including velocities at both ends of the cell. The equations of Fig. 2 that are identified with the velocities (the first and fifth equations of each block) are momentum equations; the remaining equations are mass and energy equations. We now note that the five unknowns for a given cell, say $(v_m)_{1\frac{1}{2}}$, α_2, p_2, e_2, and $(v_m)_{2\frac{1}{2}}$, are coupled only to the pressures in adjoining cells, in this case p_1 and p_3. Thus, if the pressures in adjacent mesh cells are held fixed, one can determine

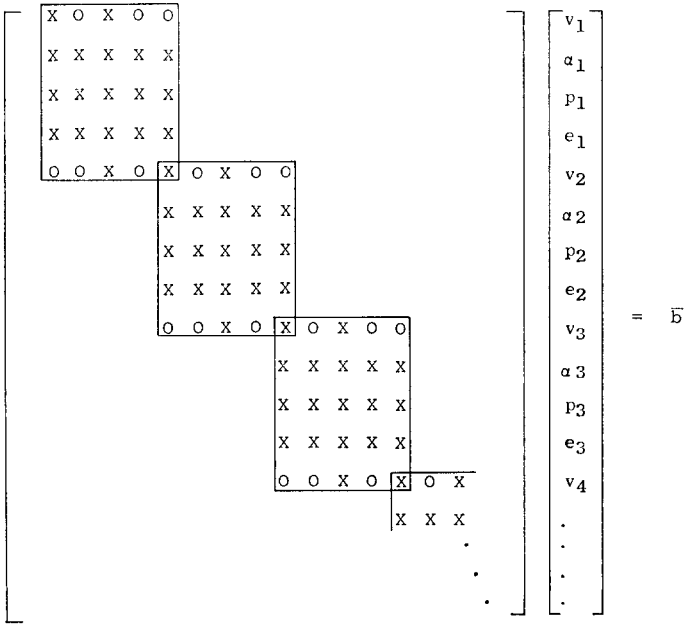

FIG. 2. Structure of linear system for *NBGS* iteration.

the five fundamental unknowns associated with the current mesh cell by solving a 5×5 linear system having the structure of a single block of the matrix depicted in Fig. 2.

The third stage of the NBGS technique is performed in the following manner. A direction for sweeping the mesh is chosen; this direction can be varied in successive iterations if desired. All five variables associated with the first mesh cell are determined in the above manner using the previous iterate pressure in cell 2. Next, the cell 2 variables are updated using the new pressure in cell 1 but an old pressure in cell 3. We note that the velocity on the boundary between cells 1 and 2 is updated twice, once with cell1 and again with cell 2. We continue this process until all fundamental variables in all cells have been updated. This completes the third step of the iteration.

The fourth stage of the NBGS iteration proceeds in the following manner. Having obtained new values for the fundamental variables in the above manner, we complete the iteration by updating the remaining unknowns. This final procedure depends upon the precise form of the constitutive equations; in what follows we assume that an equal-temperature constraint has been imposed on the liquid and vapor. First, having p and e_l, we can obtain ρ_l and T_l from Eqs. (7) and (9). We then determine T_v by setting $T_v = T_l$ and obtain e_v from Eq. (12). With e_v and p now available, we can determine ρ_v from Eq. (8). Determination of the remaining variables, such as v_r, τ, and Γ, is a straightforward application of the remaining constitutive equations. Having thus obtained new values of all the dependent variables, a test for convergence is made and another iteration is performed if necessary.

We note finally that one simplification of the above procedure is possible. Because the momentum equations of Fig. 2 couple only a single velocity and two pressures, these equations can be used to eliminate the velocities from this set of equations in favor of the pressures. If this is done, a matrix equation having the structure shown

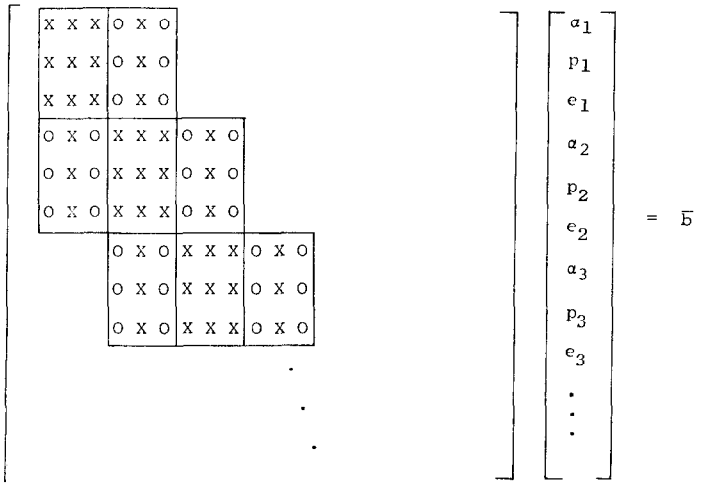

FIG. 3. Structure of simplified linear system.

in Fig. 3 is obtained. This system is clearly block tridiagonal with 3×3 blocks. If the coefficient matrix M of Fig. 3 is factored as

$$M = L + D + U, \tag{38}$$

where L and U are block lower and upper triangular matrices and D contains the diagonal blocks of M, then stage 3 of the NBGS iteration is equivalent to solving the equation

$$(L + D)\,\overline{W}^{k+1} = (U)\,\overline{W}^{k} + \overline{b}, \tag{39}$$

where $\overline{W}$ is the vector of unknowns appearing in Fig. 3. The matrix $(L + D)$ appearing in Eq. (39) is particularly easy to invert, involving only the inversion of the 3×3 diagonal blocks at each mesh cell.

It is, of course, possible to invert the full matrix M at each stage of the iteration by using a block tridiagonal matrix inversion routine. In this case, the technique becomes formally equivalent to a Newton iteration on a particular nonlinear system of equations. In more than one space dimension, or in a complicated flow network, however, the matrix M becomes more complicated and direct inversion becomes less feasible. The NBGS technique extends straightforwardly to two or three dimensions. In two dimensions, for example, the matrix M becomes block block tridiagonal with 3×3 blocks and can again be factored as in Eq. (38). The matrix $(L + D)$ is again easily inverted by solving a 3×3 system for each mesh cell.

In the present work, analytic fits to the steam tables are used for the thermal and caloric equations of state. The functions for ρ and e must be continuous but the first derivatives can be (and in the present version are) discontinuous at certain points. Some of the derivatives must also be nonzero if a solution is to exist for both the two-phase and single-phase situations. Here single phase means $\alpha = 0$ or $\alpha = 1$. For example, in the single-phase liquid case ($\alpha = 0$) the liquid density cannot be a constant independent of p and e_l. However, realistic compressibility of the fluid and a thermal expansion based on the Keenan and Keyes steam tables [3] is sufficient to prevent the matrices from becoming ill-conditioned. Examination of the matrices shows that the system becomes ill-conditioned as $\rho_l \to \rho_v$. This corresponds to the situation close to or above the thermodynamic critical point and physically implies that one is trying to calculate a void fraction for a mixture of two indistinguishable materials. For the reactor systems that we have considered no problems occur since conditions are always below the critical point.

One final note on the caloric and thermal equations of state should be made. Tabular equations of state can be used for the properties of the two phases. However, in a thermodynamic nonequilibrium code, pressure and temperature are not simple functions of one another when the phases coexist, as they are under a full-equilibrium assumption. Since an arbitrary degree of nonequilibrium (superheated liquid, for example) is to be allowed, an equation-of-state routine based on tabular data must be prepared to extrapolate beyond the range of the data if necessary. This is physically justified for moderate degrees of metastability and is one of the fundamental postulates of most nonequilibrium two-phase flow work [9].

5. Numerical Results

A wide variety of flow situations have been run successfully using the numerical methods described. While the problems have ranged from single-phase, one-dimensional flow in loops to three-dimensional, two-phase wave propagation, two simple one-dimensional examples are presented in this section. The first example is an oscillating U-tube manometer. This calculation demonstrates not only that kinematic shocks (contact discontinuities) do not disturb the solution procedure but that the drift terms can be used in a reasonably physical way to sharpen interfaces between liquid and vapor. The drift terms can have much the same effect as a flux-corrected transport procedure [10]. The second problem described is the single-ended two-phase blowdown of a long straight pipe. The convergence test for both problems was based on a relative variation of pressure and velocity between successive iterations. We have typically used a convergence criterion of 10^{-3}. For this criterion and the time step sizes indicated below, the average number of iterations for both problems was about two per time step. This is not unusual; a large number of other problems have been run with convergence tests of between 10^{-3} and 10^{-4} on either pressure or pressure and velocity with an average iteration count ranging between one and three.

A. *The Manometer*

A U-tube manometer was modeled using ten 0.1-m cells. Seven of these cells were filled with liquid; the other three contained vapor. Figure 4 illustrates both the geometry and the initial void distribution for the problem. The initial pressures for cells 1 through 8 were calculated from hydrostatic considerations. The pressures in cells 9 and 10 were atmospheric, as was the pressure in the region outside of the manometer. The initial velocities were zero. This simulates a situation in which a pressure force is applied to the right-hand side of the manometer to force the liquid up on the left side. This force is then released at $t = 0$. For this problem, the phase change rate Γ, the wall friction term τ, and the heat source q were all set to zero, although the vapor equations of state were those of steam rather than air.

The liquid thermal equation of state $\rho_l = \rho_l(p, T_l)$ was the complete expression

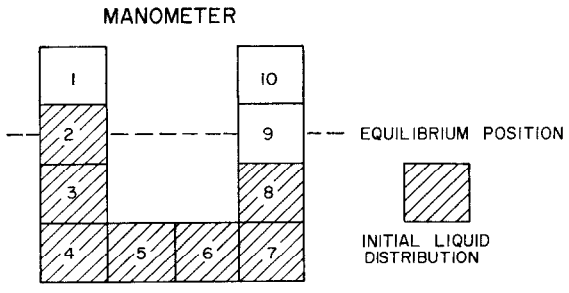

Fig. 4. Geometrical configuration for manometer problem.

(neglecting the graphical term) described in the steam tables by Keenan and Keyes [7]. A simple ideal gas equation of state was used for the vapor with a gas constant of 330 (N m/K Kg). Linear caloric equations of state were used for both the vapor and liquid, specifically

$$e_v = 667(T_v - 273.) + 2.42 \times 10^6,$$
$$e_l = 4434(T_l - 273.) - 6.24 \times 10^{-1}.$$

These represent crude approximations to the steam properties over a limited range of pressures and temperatures.

A time step of 1 msec was employed for 1.5 sec of real time. While larger time steps could have been taken, it was felt that it was desirable to see just how accurately the present type of Eulerian code could predict this problem. Runs were made both with a simple bubble rise drift model (Zuber and Hench [11]) and with a homogeneous assumption ($v_r = 0$).

Figure 5 shows a comparison of the computed and analytic liquid velocities for one period of the manometer with the bubble rise drift model. Figure 6 illustrates how the employment of the drift-flux model can be used to sharpen interfaces. After 1.5 sec the homogeneous run has suffered from noticeable diffusion while the run with drift retains a much sharper interface. These results show that this method is capable of producing reasonable results for problems in which interfaces are present.

B. *The Blowdown*

The second problem involves the blowdown of a single long constant-area pipe. The dimension and initial conditions approximate those of Edward's pipe blowdown [12, 13]. Specifically the initial subcooled liquid was at 503 K and 6.7 MPa. At $t = 0$ the pressure at the open end of the pipe is set to atmospheric pressure while the fluxes at the closed end remain at zero.

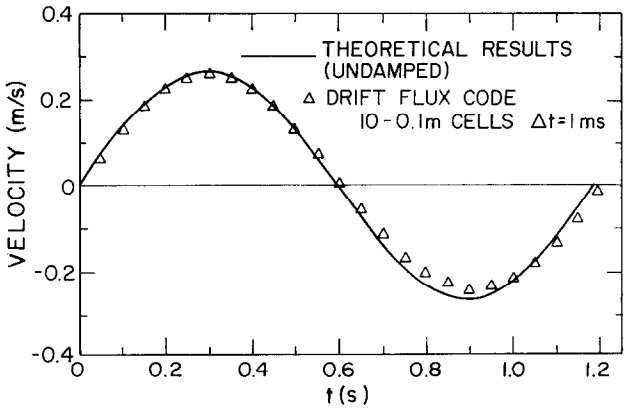

FIG. 5. A comparison of analytical and computational results for manometer problem.

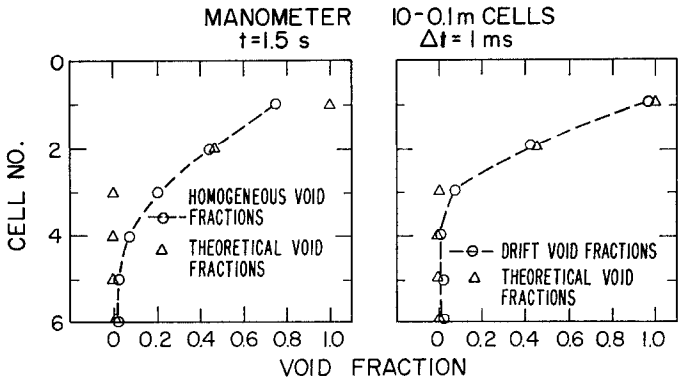

FIG. 6. A demonstration of the effect of drift on the sharpness of interfaces.

For this problem the pipe was represented as 41 mesh cells with $\Delta z = 0.1$ m. A constant time step of 0.1 msec was used to run out the solution.

The thermodynamic equations of state used for the calculation were identical to those described for the manometer while the wall friction term was based on a suggestion by Hirt and Romero [14]. The flashing model is a Nigmatulin form proposed by Rivard and Torrey [15]. Specifically the phase change term is composed of an evaporation and a condensation term as indicated below:

$$\Gamma_e = \lambda_e A \rho_l \alpha (1 - \alpha)(R_{gas} T_s)^{1/2} \frac{(T_l - T_s)}{T_s},$$

$$\Gamma_c = \lambda_c A \rho_v \alpha (1 - \alpha)(R_{gas} T_s)^{1/2} \frac{(T_v - T_s)}{T_s},$$

$$\lambda_e = 0.1, \quad T_l \geqslant T_s,$$
$$= 0.0, \quad T_l < T_s;$$

$$\lambda_c = 0.1, \quad T_v \leqslant T_s,$$
$$= 0.0, \quad T_v > T_s;$$

$$A = (\tfrac{4}{3} N\alpha)^{2/3}, \qquad \alpha \leqslant 0.5,$$

$$= (\tfrac{4}{3} N(1 - \alpha))^{23/}, \qquad \alpha > 0.5.$$

The N appearing above is the number of bubbles per cubic meter and is taken to be 1.0×10^7. The gas constant R_{gas} is set to 462.

In the drift-flux code the phase change was expressed as

$$\Gamma = C_e \left\{ \lambda_e (1 - \alpha) \frac{(T_l - T_s)}{(T_s)^{1/2}} \right\}^{n+1} + C_c \left\{ \lambda_c \alpha \frac{(T_v - T_s)}{(T_s)^{1/2}} \right\}^{n+1},$$

where

$$C_e = A^n \rho_l{}^n \alpha^n (R_{gas})^{1/2} \quad \text{and} \quad C_c = A^n \rho_v{}^n (1 - \alpha)^n (R_{gas})^{1/2}.$$

When written in this form the phase generation rate is implicit enough to be stable and is self-limiting (i.e., if the void fraction is equal to 1 no more vaporization can occur).

No formal break model was used in the code. Quantities at the pipe exit were donor celled so that the only variable outside of the pipe which appeared in the difference scheme was the ambient pressure. This same procedure has been used by Hirt and Romero [14] for similar calculations. Questions about the validity of this technique for two-phase choked-flow situations exist; but the lack of a well-defined, accurate choking criterion for two-phase flow makes the decision to include such a break model more difficult. The results obtained with the present codes for blowdowns have proved satisfactory thus far, at least with regard to matching experimental pressures. Figures 7 and 8 display typical results for the pipe blowdown pressures very near the two ends of the pipe. The runs represented were made in a homogeneous mode ($v_r = 0$) but other results with Zuber–Findley [16] slip correlations were in substantial agreement.

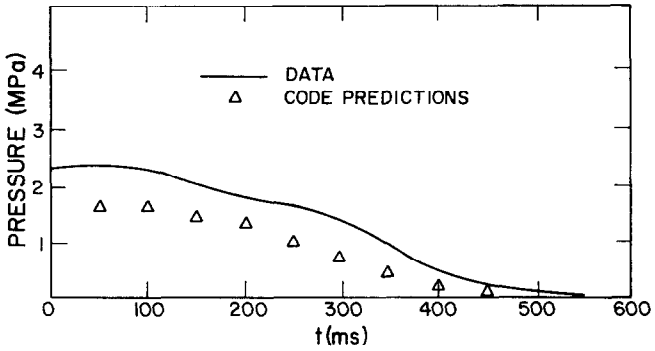

FIG. 7. Pipe blowdown pressure history at a point 0.168 m from open end.

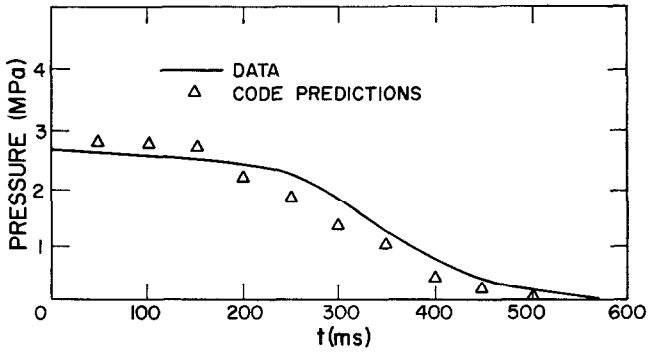

FIG. 8. Pipe blowdown pressure history at a point 0.08 m from closed end.

6. Conclusions

The NBGS technique has been applied to a wide variety of two-phase flow situations in both one- and three-space dimensions. It has proved to be reasonably accurate for the modeling purposes for which it was intended (a large systems code), but most important of all it has proved to be a more robust procedure than other solution strategies.

References

1. G. Kocomustafaogullari, "Thermo-Fluid Dynamics of Separated Two-Phase Flow," Ph.D. Thesis, School of Mechanical Engineering, Georgia Institute of Technology, 1971.
2. M. Ishii, "Thermo-Fluid Dynamic Theory of Two-Phase Flow," Eyrolles, Paris, 1975.
3. F. H. Harlow and A. A. Amsden, *J. Computational Physics* **8** (1971), 197.
4. A. A. Amsden and F. H. Harlow, "KACHINA: An Eulerian Computer Program for Multifield Fluid Flows," Los Alamos Scientific Laboratory Report LA-5680 (1975).
5. F. H. Harlow and A. A. Amsdem, *J. Computational Physics* **18** (1975), 440.
6. J. M. Ortega and W. C. Rheinboldt, "Iterative Solution of Nonlinear Equations in Several Variables," Academic Press, New York, 1970.
7. J. H. Keenan and F. G. Keyes, "Thermodynamic Properties of Steam," Wiley, New York, 1939.
8. G. E. Forsythe and W. R. Wasow, "Finite-Difference Methods for Partial Differential Equations," Wiley, New York, 1960.
9. J. P. Hirth and G. M. Pound, "Condensation and Evaporation: Nucleation and Growth Kinetics," (B. Chalmers, Ed.), Progress in Materials Science, Vol. 11, Pergamon, Oxford, 1963.
10. D. L. Book and J. P. Boris, *AIAA* (1973), 182.
11. N. Zuber and J. Hench, Report No. 62GL100, General Electric Company, Schenectady, N.Y.,
12. A. R. Edwards and T. P. O'Brian, *J. BNES* **9**, 125 (1970).
13. R. W. Garner, "Comparative Analysis of Standard Problems, Standard Problem 1," Aerojet Nuclear Company Report, Interim Report, I-212-75-5.1, October 1973.
14. C. W. Hirt and N. C. Romero, "Application of a Drift-Flux Model to Flashing in Straight Pipes," Report No. LA-6005-MS, Los Alamos Scientific Laboratory, Los Alamos, N.M., 1975.
15. W. C. Rivard and M. D. Torrey, "Numerical Calculation of Flashing from Long Pipes Using a Two-Fluid Model," Report No. LA-6104-MS, Los Alamos Scientific Laboratory, Los Alamos, N.M., 1975.
16. N. Zuber and J. Findley, "The Effects of Non-Uniform Flow Concentration Distributions and Effect of the Local Relative Velocity on the Volumetric Concentration in Two-Phase Flow," EUAREC 1096, GEAP 4592, General Electric Co., Schenectady, N.Y., 1964.